Int. J. Electrochem. Sci., 10 **(2015)** 7303 - 7319

International Journal of
ELECTROCHEMICAL
SCIENCE
www.electrochemsci.org

Response Surface Optimization of MWCNT modified Carbon Paste Electrode for Zn(II) Determination

Rimal Isaac[*], *P. K. Praseetha*

Department of Nanotechnology, Noorul Islam Centre for Higher Education (N.I. University), Kumaracoil, Thuckalay, Kanyakumari District, Tamilnadu, INDIA - 629180
[*]E-mail: rimalisaac@gmail.com

Received: 29 May 2015 / *Accepted:* 10 July 2015 / *Published:* 28 July 2015

A novel carbon paste electrode based on 3,7,12,17-Tetramethyl-8,13-divinyl-2,18-porphinedipropionic acid disodium salt (Ionophore) modified with multi-walled carbon nanotube (MWCNT) is fabricated for the selective determination of Zn^{2+}. Central composite design (CCD) and response surface methodology is used in this work to study the effect of different independent variables and to optimize the variable for a particular response. Five variables namely, ionophore, MWCNT, sodium tetraphenylborate, paraffin oil and graphite were studied in a 33 experiment CCD. The slopes of the calibration graphs were measured as the response of the electrode. A mathematical model equation was obtained from computer simulations from the optimization studies. The optimized electrode showed a linear range of 1.0×10^{-1} to 3.15×10^{-7} M and a detection limit of 2.5×10^{-7} M. The response time of the electrode was found to be 20 s and a slope of 30.73±0.81 mV/decade. The electrode showed a good selectivity for Zn^{2+} relative to many cations. Potentiometric titration was used to study the analytical application of the electrode. The optimized electrode was effectively used for the titration of Zn^{2+} with EDTA.

Keywords: carbon paste electrode; carbon nanotubes; ion selective; response surface design; zinc ion

1. INTRODUCTION

Zinc (Zn) is a metal, which forms an essential nutrient for plants, animal species and microorganisms. It is the most abundant heavy metal found in the human body. Human serum contains about 1 mg/L Zn [1]. The daily human requirement of Zn is around 15 mg [2]. Nearly 300 enzymes in the human body require Zn for its normal activities and to maintain the structure. A recent study reveals that nearly 2 billion people in the developing countries are affected by Zn deficiency [3]. The illness caused by Zn deficiency is Anorexia [4], chronic liver disease, chronic renal disease, sickle cell

disease, diabetes, malignancy, and other chronic illnesses [5]. Excess of Zn causes tremors, microcytichypo chronic anemia, fewer chills pulmonary manifestation, diarrhea and gastroenteritis [6]. Zn functions as an efficient antioxidant and anti-inflammatory agent [7-10]. In industries, the uses of Zn include galvanizing, die castings and in alloys. The oxide of Zn is used in paints, cosmetics, pharmaceuticals, soaps and textiles. Excess of Zn in the environment can be a serious environmental pollution by decreasing the amount of microorganisms in the soil [11, 12]. This Zn causes contamination of food and agricultural wastes [13]. Because of the above said facts it is essential to develop more sensitive, accurate and analytical techniques to detect trace levels of Zn in the fields of medicine and environment.

There are many analytical methods available for the estimation of Zn, including potentiometry [14], flame atomic absorption spectrometry [15], UV-Vis spectroscopy [16], fluorescence methods [17] and inductively coupled plasma atomic emission spectrometry (ICPAES) [18]. The electronic configuration of Zn is $1s^2 2s^2 2p^6 3s^2 3p^6 3d^{10} 4s^2$, which shows a completely filled d-orbital thereby making it not suitable for techniques that require spectroscopic or magnetic signals [19]. Among these analytical techniques, potentiometric technique involving ion-selective electrodes (ISEs) offer better response, selectivity and repeatability in a cost effective manner. There are many ISEs employing polymeric membrane were developed for the determination of Zn [6, 19-29]. The ISEs employ a key component known as the ionophore, which interacts with the metal of interest forming a selective complex, thereby defines the sensitivity and selectivity of the system.

Over ISEs, Carbon paste electrodes (CPEs) are having more advantages like low ohmic resistance, stable response, renewability and there is no need of an internal solution. Carbon paste is made from graphite and mineral oil. In recent years, carbon nanotubes (CNTs) are extensively used in CPEs [30-33]. CNTs are a good candidate because of their ultra-light weight, high electrical conductivity, high aspect ratio, high mechanical strength, high thermal conductivity and high surface area [34].

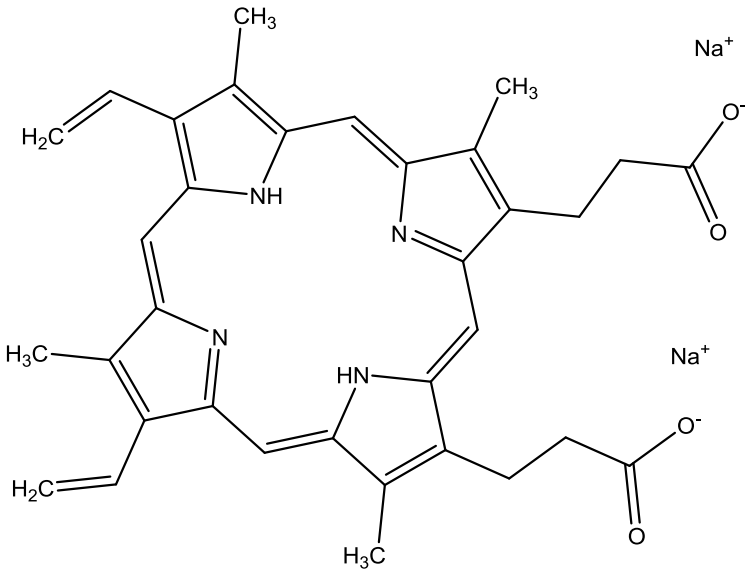

Figure 1. Chemical structure of protoporphyrin IX disodium (3,7,12,17-Tetramethyl-8,13-divinyl-2,18-porphinedipropionic acid disodium salt)

In this present work, protoporphyrin IX disodium salt is used as the ionophore in a CPE modified with multi-walled CNT (MWCNT). The chemical structure of ionophore is given in fig. 1. In a previously reported study, the ionophore used was applied for the fabrication of Zn ion (Zn(II)) PVC membrane sensor [29]. The effects of individual variable used for the fabrication of CPE for the detection of Zn(II) such as the amounts of ionophore, sodium tetraphenylborate (NaTPB), graphite powder, paraffin oil and MWCNT were studied and the variables were optimized by using central composite design (CCD) under response surface methodology (RSM) by running least number of experiments.

2. EXPERIMENTAL

2.1. Materials

All the chemicals used were of the analytical grade and used as such without purification. All the solutions of the cations were prepared from the analytical grade of the corresponding chloride salt. Ultra-pure water is used for the preparation of salt solutions (Milli–Q System; Millipore Corp.). Graphite, sodium hydroxide and paraffin oil was purchased from Merck, Mumbai. MWCNT was purchased from United Nanotech Innovations Pvt. Ltd., Bangalore, India. Protoporphyrin IX disodium salt and Zinc chloride from Sigma Aldrich. Potassium chloride, manganous chloride and barium chloride were purchased from Spectrum chemicals, Cochin. Ammonium chloride, copper(II) chloride, Ethylenediaminetetraacetic acid disodium salt and NaTPB from Himedia, Mumbai. Sodium chloride and silver chloride from Loba chemie Pvt Ltd, Mumbai. Ferrous chloride and hydrochloric acid from NICE chemicals, Kochi. Tetrahydrofuran (THF) from High Purity Laboratory Chemicals Pvt. Ltd., Mumbai. Stannous chloride and cobalt chloride from Thomas Baker chemicals private Ltd, Mumbai.

2.2. Electrode fabrication

A polyethylene syringe (4 mm i.d., 1 ml), the tip is cut off with a blade is used as the electrode body to fill the modified carbon paste. Electrical contact was made using an unmodified carbon paste-copper wire contact. Different amounts of graphite, ionophore, NaTPB, MWCNT and 7-10 mL THF were mixed in a 25 mL beaker. The mixture was mixed thoroughly by sonication method or sometimes by spatula for 15 min. Then the THF is allowed to evaporate completely at room temperature. Now paraffin oil is added to the mixture and carefully hand mixed in an agate mortar and pestle to form a homogenous paste. This paste is packed into the hole of the electrode body and the surface is polished against a white paper until the surface is having a shiny appearance. The surface of the electrode is renewed before each set of measurement. It is used directly for potentiometric measurement without preconditioning.

2.3. Potential measurement and selectivity coefficient determination

A homemade potentiometer coupled to a digital multimeter is used for the potential measurements [35]. pH measurements were made using a Medox Bio pH Meter. All the measurements were conducted at 25±0.1°C. Ag|AgCl electrode is used as the reference electrode for potential measurements. The potential measurements were done by using the following scheme of cell assembly:

Ag|AgCl, KCl (satd.) || test solution | CPE | Cu

The selectivity coefficient of the prepared electrode was determined by using fixed interference method [36]. In this method, the activity of the interfering ion (a_B, 1.0 x 10^{-2}) is kept constant and varying the activity of primary ion (a_A) by using the following equation:

$$K_{A,B}^{pot} = {a_A}\Big/{(a_B)^{z_A/z_B}} \quad (1)$$

z_a and z_b are the charges of the primary ion, A and the secondary ion, B. Both z_A and z_B has the same sign whether positive or negative.

2.4. Central Composite Design

CCD was used to optimize the independent factors, namely ionophore (X_1), paraffin oil (X_2), NaTPB (X_3), graphite (X_4) and MWCNT (X_5) at five levels and 7 replicates (designed in Minitab 17) at the center point and are presented in table 1. The model equation can be expressed as

$$y = \beta_0 + \sum_{i=1}^{5} \beta_i x_i + \sum_{i=1}^{5} \sum_{j=1}^{5} \beta_{ij} x_i x_j + \sum_{i=1}^{5} \beta_{ii} x_i^2 \quad (2)$$

Where y is the predicted response (slope), x_i's and x_j's are the independent variable and β_0, β_i's, β_{ij}'s, β_{ii}'s are the model constant, linear coefficients, interaction coefficients and quadratic coefficients respectively.

The effect of each of the factors on the response can be obtained using RSM technique. It also allows to investigate the levels of the factors to which it affects the response. The results were analyzed by three-dimensional surface response, analysis of variance (ANOVA) and desirability function (DF). The significant terms were chosen on the basis of p value ($p < 0.05$), all the other terms were eliminated from the model using a backward elimination process.

Table 1. Factors and levels used in the Central Composite Design

Factors	Levels				
	Low (-1)	Central (0)	High (+1)	-α	+α
X_1: Ionophore (mg)	4	6	8	2	10
X_2: Paraffin (drop)	3	5	7	1	9
X_3: NaTPB (mg)	2	4	6	0	8
X_4:Graphite (mg)	150	200	250	100	300
X_5: MWCNT (mg)	10	15	20	5	25

3. RESULT AND DISCUSSION

3.1. Central composite experimental design

The effects of the five independent variables namely, ionophore (X_1), paraffin oil (X_2), NaTPB (X_3), graphite (X_4) and MWCNT (X_5) was studied by measuring the response of each electrode. Table 2 shows the individual responses of the prepared electrode. ANOVA was carried out to study the effects of the variables involved and to validate the results obtained by CCD. The statistical significance of the variables is identified based on the p-value, $p < 0.05$ is considered statistically significant at 95% confidence interval. ANOVA results are presented in table 3. The comparison between variation from the model and the variation due to residual error is performed by Fisher's *F*-test. It is the ratio between mean square of the model and the residual error [37]. The *F*-value obtained from table 3 as 133.25 is greater (2.41 at 95% significance) than the value found in the standard *F*-table. This shows the high fitting of the model.

Table 2. List of experiments in the central composite design (uncoded values) and their responses

Trial number	Factor levels					Response	
	X_1	X_2	X_3	X_4	X_5	Slope (mV)	
						Observed	Predicted
1	4	3	2	250	10	13.88	12.91
2	8	7	6	250	20	16.33	16.38
3	8	3	2	150	10	22.45	21.84
4	4	7	2	250	20	39.42	39.11
5	4	7	6	150	20	41.22	41.48
6	8	7	6	150	10	45.12	45.65
7[a]	6	5	4	200	15	26.39	27.03
8[a]	6	5	4	200	15	27.08	27.03
9	4	3	2	150	20	8.55	7.67
10[a]	6	5	4	200	15	24.44	27.03
11[a]	6	5	4	200	15	28.55	27.03
12	4	3	6	150	10	22.45	22.58
13	8	3	6	150	20	33.44	33.45
14	8	7	2	250	10	45.74	45.70
15	4	7	2	150	10	16.22	16.39
16	8	3	6	250	10	46.2	46.12
17	8	7	2	150	20	19.25	19.30
18[a]	6	5	4	200	15	29.23	27.03
19	4	7	6	250	10	42.15	42.32
20	4	3	6	250	20	14.56	14.21
21	8	3	2	250	20	49.7	48.61
22[a]	6	5	4	200	15	26.45	27.03
23	2	5	4	200	15	34.85	35.37

24	6	5	4	100	15	24.45	24.26
25	6	5	4	200	25	22.18	22.87
26	6	1	4	200	15	14.45	16.00
27[a]	6	5	4	200	15	27.67	27.03
28	10	5	4	200	15	55.23	55.46
29	6	9	4	200	15	31.55	30.74
30	6	5	4	300	15	37.57	38.51
31	6	5	8	200	15	25.32	24.59
32	6	5	0	200	15	10.45	11.92
33	6	5	4	200	5	31.29	31.19
[a]7 replicates of center point							

From the ANOVA results all the factors are more significant ($P < 0.001$) in the response of the electrode. The regression coefficients and the regression equation for the model is given in table 4. The positive and negative signs in the regression equation show the synergistic and antagonistic effect of the variables [38]. From the regression equation, all the factors are having positive signs, this shows the synergistic effect of the variables on the response. The suitability of the polynomial equation is determined by the values of regression coefficient ($R^2 = 0.9942$ and adjusted $R^2 = 0.9867$) which shows good distribution of result around the mean. The fitting between the observed slope and the predicted slope is presented in fig. 2 and it shows a good correlation with the experimental data ($R^2 = 0.99$), which shows that the model can be applied to explain the experimental data.

Table 3. Analysis of Variance for slope

Source of Variation	Degrees of Freedom	Sum of Squares	Mean Square	F-Value	P-Value
Model	18	4532.06	251.781	133.25	0.000
$\mathbf{X_1}$	1	605.41	605.412	320.41	0.000
$\mathbf{X_2}$	1	325.75	325.754	172.4	0.000
$\mathbf{X_3}$	1	240.67	240.667	127.37	0.000
$\mathbf{X_4}$	1	304.74	304.736	161.28	0.000
$\mathbf{X_5}$	1	104	104	55.04	0.000
$\mathbf{X_1*X_1}$	1	640.19	640.185	338.81	0.000
$\mathbf{X_2*X_2}$	1	25.36	25.362	13.42	0.003
$\mathbf{X_3*X_3}$	1	145.85	145.85	77.19	0.000
$\mathbf{X_4*X_4}$	1	35.88	35.876	18.99	0.001
$\mathbf{X_1*X_2}$	1	688.01	688.013	364.12	0.000
$\mathbf{X_1*X_3}$	1	91.97	91.968	48.67	0.000
$\mathbf{X_1*X_4}$	1	16.28	16.281	8.62	0.011
$\mathbf{X_1*X_5}$	1	155.25	155.252	82.16	0.000
$\mathbf{X_2*X_4}$	1	15.25	15.249	8.07	0.013
$\mathbf{X_2*X_5}$	1	73.44	73.445	38.87	0.000

X_3*X_4	1	692.48	692.479	366.48	0.000
X_3*X_5	1	297.56	297.563	157.48	0.000
X_4*X_5	1	36.54	36.542	19.34	0.001
Residual Error	14	26.45	1.890		
Lack-of-Fit	9	11.85	1.316	0.45	0.859
Pure Error	5	14.61	2.921		
Total	32				

Table 4. Characteristics of the constructed model

Response	R^2	R^2 adjustment	R^2 prediction	Regression equation
Slope	99.42%	98.67%	96.22%	Slope = -169.3 + 1.97*X_1 + 19.13*X_2 + 29.19*X_3 + 0.2393*X_4 + 5.458*X_5 + 1.1488*X_1*X_1 - 0.2287*X_2*X_2 - 0.5484*X_3*X_3 + 0.000435*X_4*X_4 - 1.6394*X_1*X_2 - 0.5994*X_1*X_3 + 0.01009*X_1*X_4 - 0.3115*X_1*X_5 - 0.00976*X_2*X_4 - 0.2142*X_2*X_5 - 0.06579*X_3*X_4 - 0.4313*X_3*X_5 - 0.00604*X_4*X_5

The response surface plots for the response slope is shown in fig. 3. The interacted factors are shown in the figure while keeping the other factors constant in the constructed model. The middle level is chosen as the constant levels. The curvature nature of the plot shows strong interaction between the variables. From the graphs it is evident that all the factors affect the response of the model. Also in order to study the effect of the factors on the response, Pareto analysis was carried out [39]. Pareto analysis calculates the percentage effect (P_i) of the different factors on the response based on the following equation:

$$P_i = \left(\frac{\beta_i^2}{\sum_{i=1}^{18} \beta_i^2} \right) x\ 100\ (i \neq 0) \quad (3)$$

where β_i is the coefficient of regression of the individual variables.

The Pareto analysis result is shown in fig. 4. From the graph, the factors NaTPB (67.79%), paraffin oil (29.11%), MWCNT (2.37%) and ionophore (0.31%) are the important factors that causes the main effect on the slope.

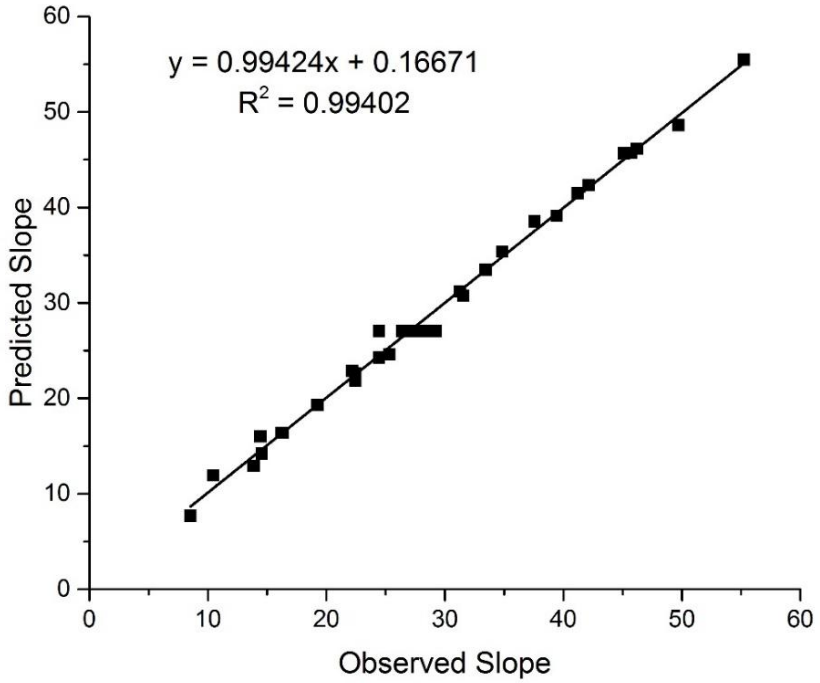

Figure 2. Plot of observed slope vs predicted slope

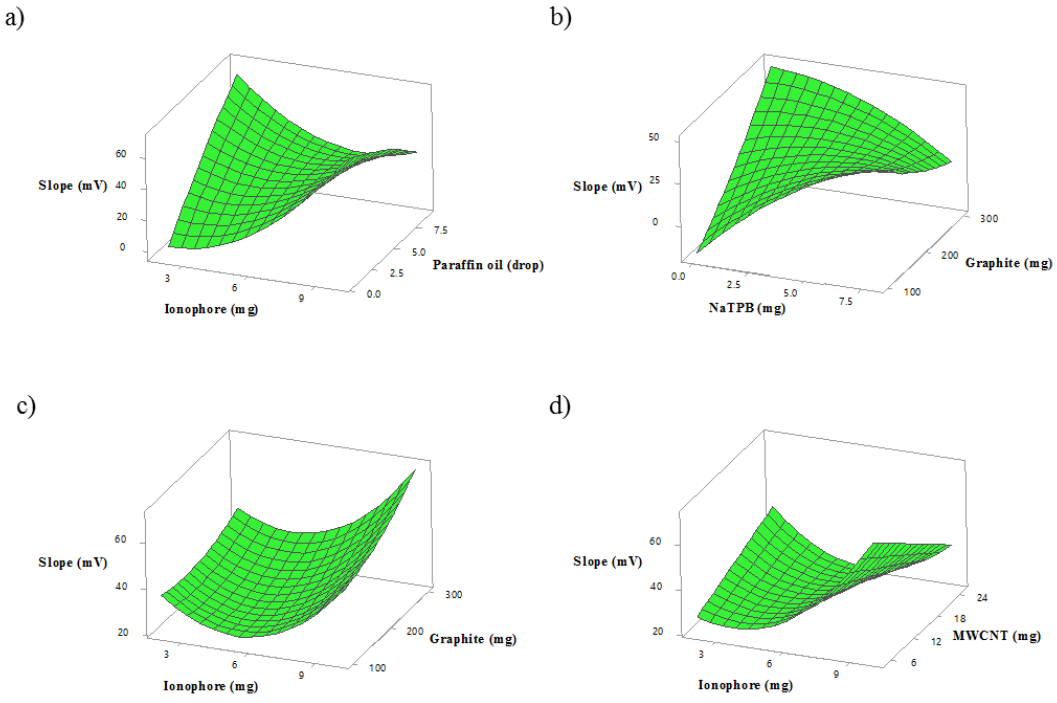

Figure 3. Response surface plots for slope: a) ionophore vs paraffin oil; b) NaTPB vs graphite; c) ionophore vs graphite and d) ionophore vs MWCNT.

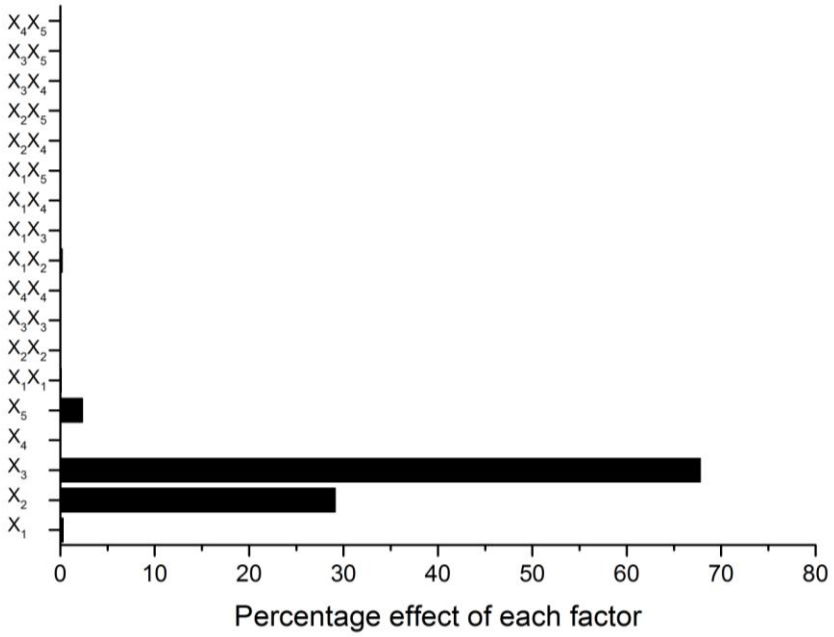

Figure 4. Percentage effect of factors by Pareto analysis

3.2. Optimization of design

The response optimizer option under Minitab with desirable function is used for the optimization of the process. A scale in the range of 0.0 (undesirable) to 1.0 (desirable) was used to optimize the process. The optimal condition (Fig. 5) at which the slope was 29.55 mV/decade was found to be as ionophore (9.9832 mg), paraffin oil (drop) (9), NaTPB (7.9642 mg), graphite (100 mg) and MWCNT (19.2234 mg). Running the experiments with the optimum values resulted in a slope of 31.91 mV, validating the model.

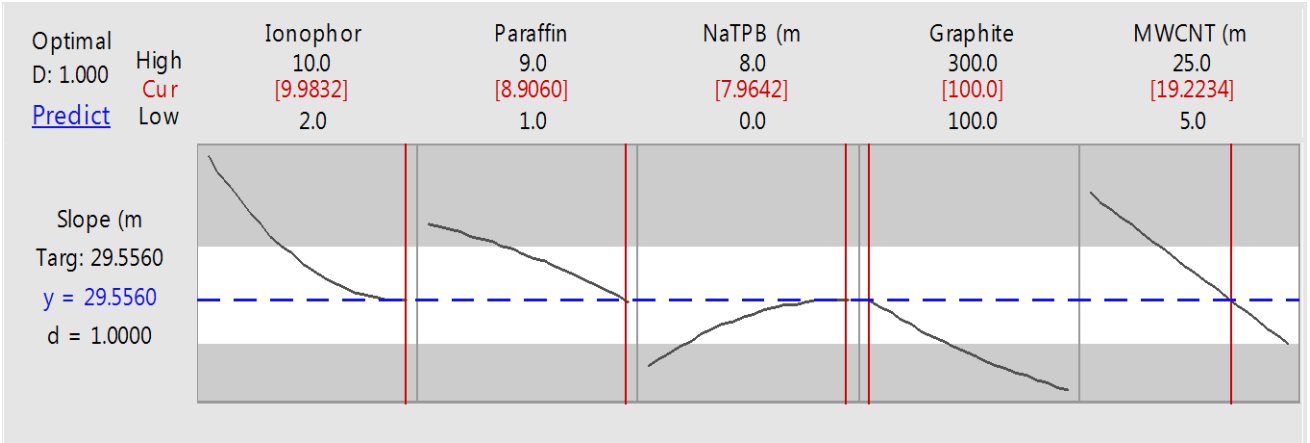

Figure 5. Profile of desirability function for the predicted values.

3.3. Emf response and effect of pH

The performance characteristics of the prepared electrode was studied based on the recommendations from IUPAC [40]. The response of the electrode towards various metal ions are studied within the concentration range of 1.0 x 10^{-1} M to 1.0 X 10^{-8} M as shown in fig. 6. From the graph it is clear that the electrode showed a Nernstian slope from Zn^{2+} and poor response for other ions. The calibration graph of the electrode is given in fig. 7. The working linear concentration range of the electrode was found to be 1.0 x 10^{-1} M to 3.15 x 10^{-7} M. in this range the electrode showed a Nernstian slope of 31.91 mV $decade^{-1}$. The detection limit of the electrode was calculated from the calibration graph from the intersection of two extrapolated linear segments and was found to be 2.5 x 10^{-7} M.

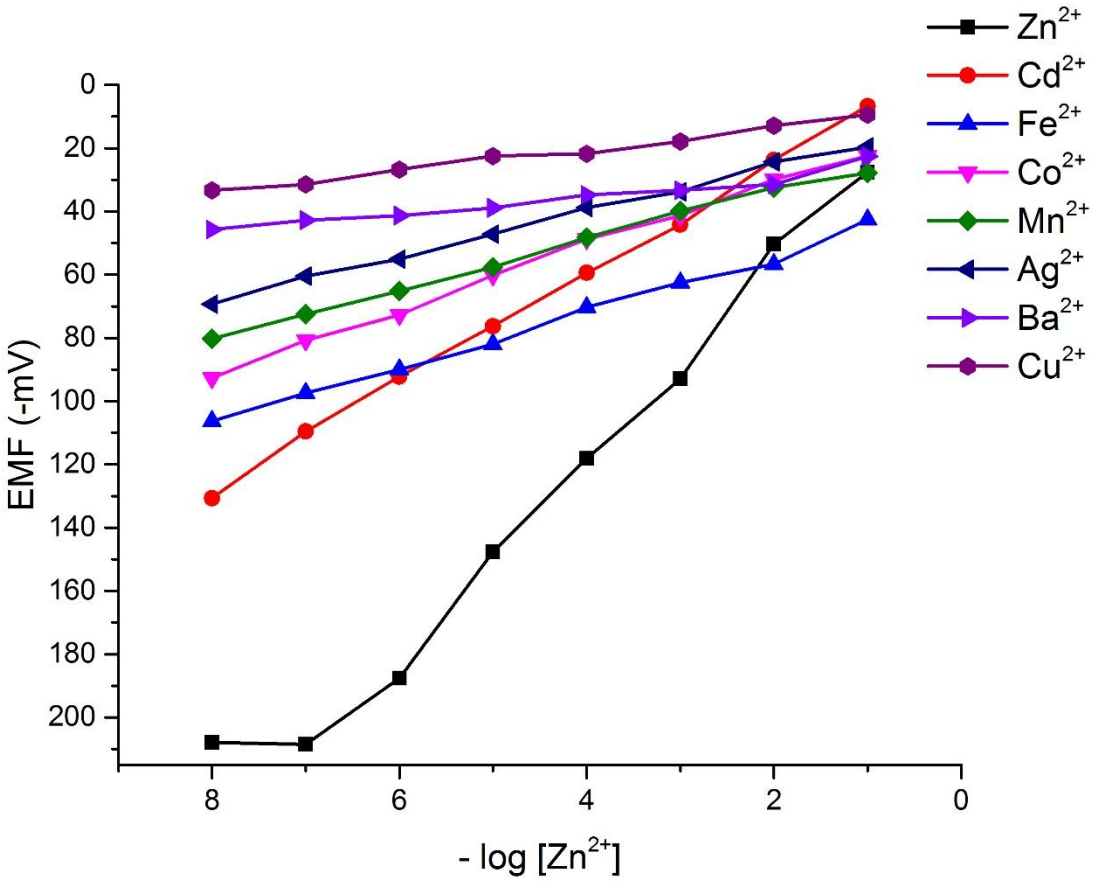

Figure 6. Potential response of the optimized electrode to difference cations.

The effect of pH on the electrode was studies by measuring the emf at a fixed Zn concentration (1.0 x 10^{-3} M) in different pH solutions. pH of the solution was varied from 1.0 to 8.5 by the addition of hydrochloric acid (0.1 M) or sodium hydroxide (0.1 M). Fig. 8 shows the potential variation with respect to change in pH. The optimized electrode composition was used for all the studies. The electrode showed a stable response in the pH range of 2.7 to 7.0. In this region the electrode found no interference from either OH^- or H^+ ions. At higher pH the deviation from a stable value may be caused

from the formation of Zn^{2+} ion hydroxyl complexes and at lower pH the deviation may be caused by the partial protonation of the ionophore [41, 42].

3.4. Selectivity coefficient evaluation

The response of any ion selective electrode for a primary ion in the presence of other ions is expressed as potentiometric selectivity coefficient. It gives the basic information of interferences in an ion selective electrode response. The selective coefficient is determined by fixed interference method by using eqn. (1) at a fixed concentration of foreign ions (1.0×10^{-2} M) and varying the concentration of Zn^{2+} ions. The graphically calculated selectivity coefficient values are given in table 5.

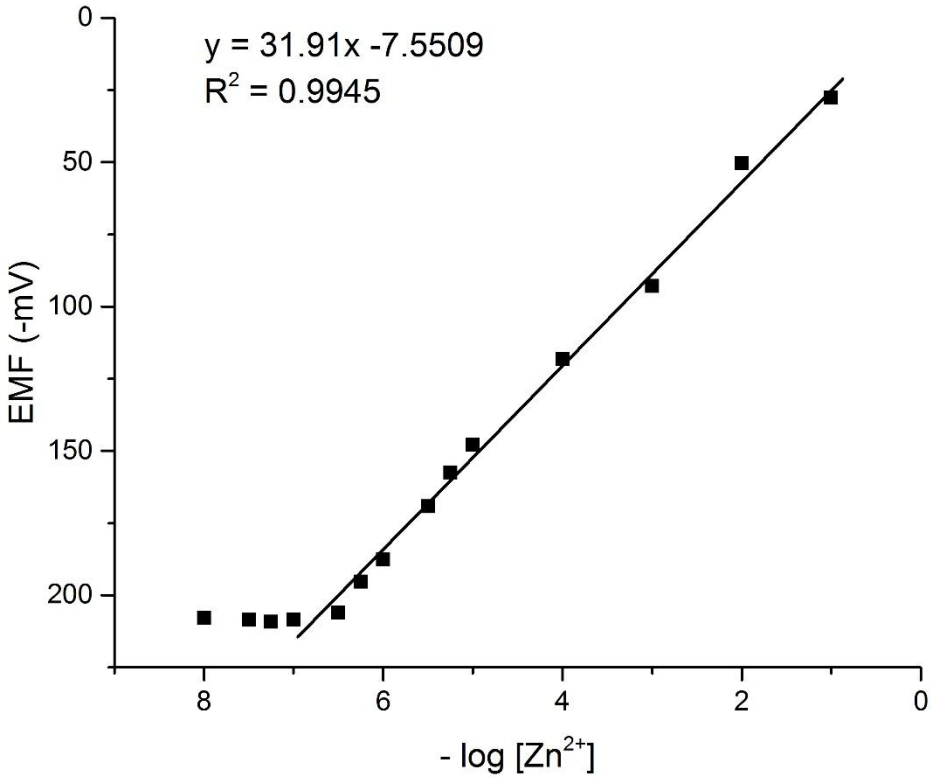

Figure 7. Calibration graph of the optimized electrode for the detection of Zn^{2+}.

By examining the selectivity coefficient, the optimized electrode can be used for the detection of Zn^{2+} with good selectivity in the presence of Co^{2+}, Fe^{2+}, Cu^{2+}, Sn^{2+}, K^{+}, Ag^{+}, Mn^{2+}, Ba^{2+} and NH^{4+} but it shows moderate selectivity in the presence of Na^{+}. The selectivity coefficient values for Na^{+} is relatively high, in order to at what concentration of Na^{+} the interference is high, some mixed run experiments were carried out and it is shown in fig. 9. When the concentration of Na^{+} is $\leq 1.0 \times 10^{-5}$ M it does not cause much change to the original plot of Zn^{2+}, hence the electrode can tolerate Na^{+} up to this limit.

Table 5. Potentiometric selectivity coefficient values determined using fixed interference method for the optimized electrode.

Interfering ions (B)	Selectivity Coefficient $K^{pot}_{Zn^{2+},B}$
Co^{2+}	8.4×10^{-2}
Fe^{2+}	9.2×10^{-3}
Cu^{2+}	4.6×10^{-2}
Sn^{2+}	7.2×10^{-3}
Na^{+}	6.3×10^{-1}
K^{+}	3.6×10^{-2}
Ag^{+}	5.2×10^{-2}
Mn^{2+}	4.5×10^{-3}
Ba^{2+}	9.9×10^{-3}
NH^{4+}	4.6×10^{-2}

3.5. Response time, repeatability, reproducibility and lifetime

For any analytical application of the electrode, the response characteristics are very important. Response time is the time required to reach 90% of the final equilibrium values after immersion in a series of altered concentration of Zn^{2+} solutions, each having a tenfold difference in concentration. The prepared electrode showed a response time less than 20 s over all concentration ranges. The repeatability was recorded by measuring the concentration of Zn^{2+} in 1.0×10^{-3} M solution for several times (N = 3). The relative standard deviation was ± 1.65 mV. This shows the electrode response is highly repeatable. Five similar electrodes were prepared and their reproducibility was checked at optimum (table 6). The slope was found to be 30.73±0.81 mV/decade that strongly shows that the electrode response is reproducible. The electrode response was checked for a period of 4 weeks. Over these period the response was obtained without any considerable change.

Table 6. The reproducibility of the electrode response at optimum composition.

Electrode	Slope[a]	Correlation coefficient	Linear Range[b]
1	31.91	0.994	0.1-0.31
2	30.50	0.998	0.1-0.31
3	31.14	0.998	0.1-0.31
4	30.34	0.996	0.1-0.63
5	29.77	0.993	0.1-0.31
RSD = ±0.81	Average slope = 30.73	Average = 0.995	
[a]mV/decade concentration			
[b]Linear range (M-µM)			

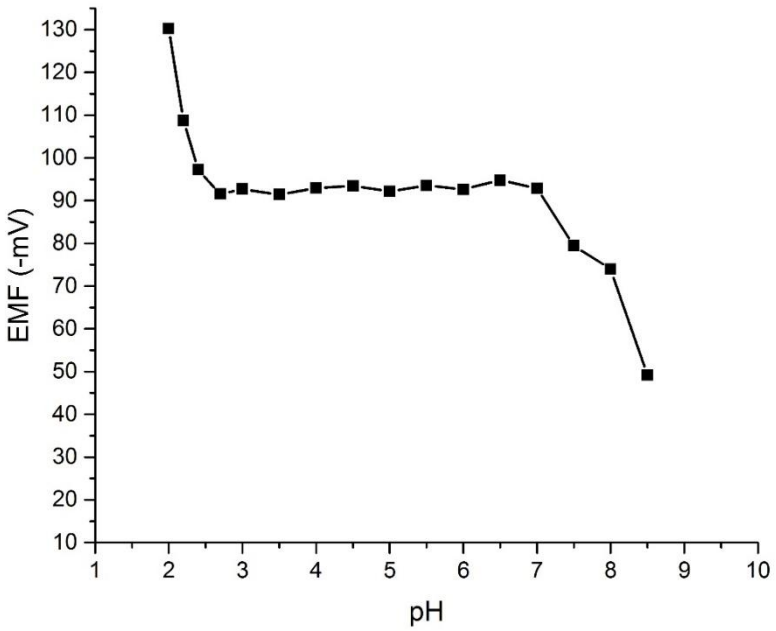

Figure 8. Effect of pH on the response of optimized electrode; $[Zn^{2+}] = 1.0 \times 10^{-3}$ M.

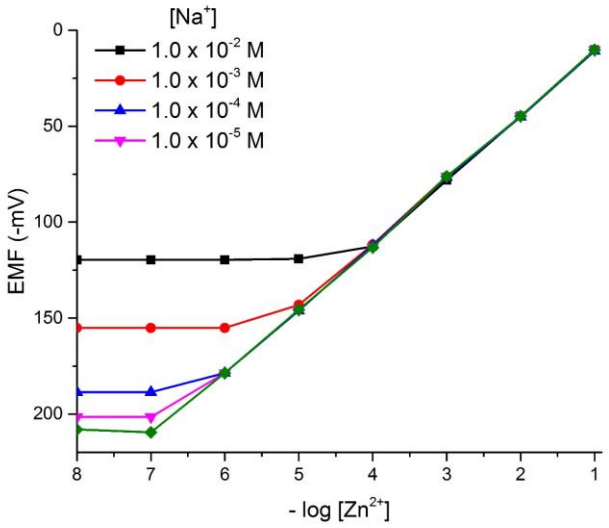

Figure 9. Variation of potential with Zn^{2+} concentration in the presence of different concentration of Na^{+}.

3.6. Analytical application

Analytical application was performed by using the prepared electrode as an indicator electrode for the potentiometric titration of Zn^{2+} against EDTA. The potentiometric titration was performed by titrating 1.0×10^{-3} M Zn^{2+} solution against 1.0×10^{-2} EDTA solution. The potentiometric titration result is shown in fig. 10. A non-sigmoidal graph is obtained this may be due to the interference of Na^{+}

ions from the used di-sodium EDTA salt [43]. However the sharp breakpoint in the graph corresponds to the potentiometric determination of Zn^{2+}.

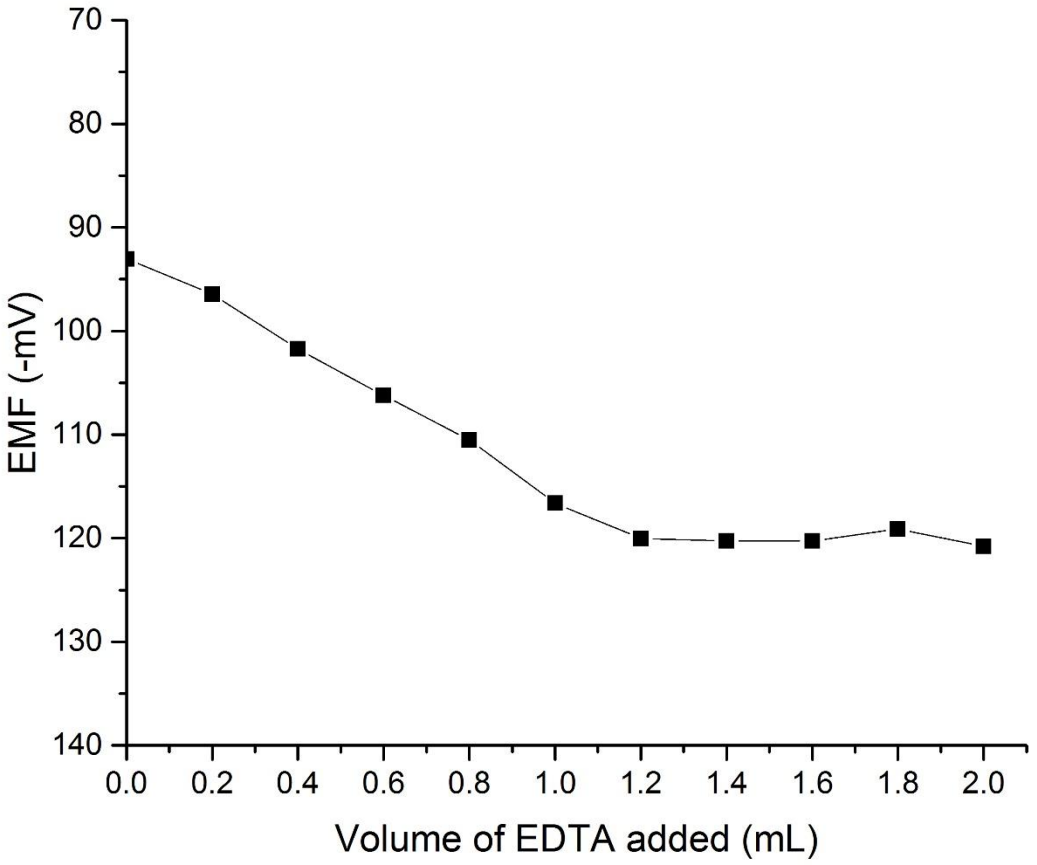

Figure 10. Potentiometric titration curve for Zn^{2+} (1.0×10^{-3}, 10 mL) against EDTA (1.0×10^{-2}) using the prepared optimized electrode as an indicator electrode.

Table 7. Comparison of the analytical characteristics of Zn selective electrodes

Ionophore	Slope[a]	L.R.[b]	R.T.[c]	D.L.[d]	Reference
Zn-bis(2,4,4-trimethylpentyl)dithiophosphinic	30.1	2.8×10^{-5} - 1.0×10^{-1}	15	-	[44]
4-tert-butylcalix[4]arene	28.0 ± 1.0	9.8×10^{-6} - 1.0×10^{-1}	30	5.0×10^{-7}	[45]
N,N′-bis(acetylacetone)ethylenediimine	30.0	1.0×10^{-6} - 1.0×10^{-1}	15	-	[23]
N,N′-phenylenebis (salicylideaminato)	29.4 ± 0.2	5.0×10^{-7} - 1.0×10^{-1}	<10	2.6×10^{-7}	[26]
18-crown-6, dibenzo 18-crown-6	30.0 29.0	1.0×10^{-5} – 1.0×10^{-1}	≤15	1.5×10^{-6} 7.5×10^{-6}	[46]
2,6-Diacetylpyridinebis(benzenesulfonylhydrazide)	29.06 ± 0.1	1.0×10^{-6} - 1.0×10^{-1}	20	1.0×10^{-7}	[25]
3,7,12,17-Tetramethyl-8,13-divinyl-2,18-porphine-dipropionic acid in PVC membrane electrode	30.0	1.3×10^{-5} - 1.0×10^{-1}	10	-	[29]
12-crown-4	29.5 ± 1.0	7.0×10^{-5} – 1.0×10^{-1}	< 10	-	[47]
6,7:14,15-Bzo_2-10,11-(4-methylbenzene)-[15]-6,14-diene-9,12-dimethylacrylate-	28.8 ± 0.3	5.0×10^{-7} - 1.0×10^{-2}	12	3.3×10^{-7}	[48]

9,12-N_2-1,5-O_2					
N,N′-Bis(2-dimethylaminoethyl)-N, N′-dimethyl-9,10 anthracenedimethanamine	30.0 ± 0.5	1.0×10^{-5} - 1.0×10^{-1}	15	1.5×10^{-6}	[49]
NiO nanostructures and 12-crown-4	36.0	1.0×10^{-6} - 1.0×10^{-1}	10	5.0×10^{-7}	[19]
dimethyl-8,13-divinyl-3,7,12,17-tetramethyl-21H, 23H-porphine-2,18-dipropionate	29.0 ± 1.0	1.5×10^{-5} - 1.0×10^{-1}	10	-	[50]
1,12,14-triaza-5,8-dioxo-3(4),9(10)-dibenzoyl-1,12,14-triene	29.2 ± 0.4	1.3×10^{-7} – 1.0×10^{-1}	7	1.0×10^{-8}	[6]
1,13-diaza-2,3;11,12;15,18-tribenzo-4,7,10-trioxacyclononaoctane-14,19-dione	30.0 ± 1.0	1.0×10^{-1} – 9.0×10^{-5}	20	5.0×10^{-5}	[21]
tetra(2-aminophenyl) porphyrin	26.5	5.0×10^{-5} - 1.0×10^{-1}	10	3.0×10^{-5}	[51]
zinc salt of di(2-ethylhexyl)phosphoric acid dissolved in tri(2-ethylhexyl)phosphate	43.8	-	-	4.5 ± 0.1 pZn	[20]
N-[(ethyl-1 pyrrolidinyl-2)methyl] methoxy-2 sulfamoyl-5 benzamide	29.3	1.0×10^{-5} – 1.0×10^{-1}	20	7.0×10^{-6}	[22]
2,2,2-cryptand	22.0	2.06 ppm - 6.54×10^{3} ppm	<10	-	[52]
dibenzo-24-crown-8	29.0 ± 0. 5	9.2×10^{-5} - 1.0×10^{-1}	12	-	[43]
tetrabutyl thiuram disulfide	28.0	1.0×10^{-1} – 1.0×10^{-6}	10	4.2×10^{-7}	[24]
bis(2-nitrophenyl)disulfide	29.9 ± 0.4	2.9×10^{-7} - 3.2×10^{-2}	10	-	[53]
3,7,12,17-Tetramethyl-8,13-divinyl-2,18-porphinedipropionic acid disodium salt	30.73±0.81	1.0×10^{-1} - 3.15×10^{-7}	20	2.5×10^{-7}	This work
[a]mV per decade concentration.					
[b]Linear Range (M).					
[c]Response time (s).					
[d]Detection Limit (M).					

4. CONCLUSION

To the best of author's knowledge, this is the first time a CPE incorporating a nanomaterial is developed for Zn^{2+} ion using RSM. In this work by using CCD and subsequent RSM, the effect of different factors are analyzed and optimized. The optimized electrode showed a linear concentration range of 1.0×10^{-1} to 3.15×10^{-7} M and a detection limit of 2.5×10^{-7} M. The selectivity coefficient values for most of the ions are very small except Na^{+}. The electrode showed good response in the pH range of 2.7 to 7.0. Comparison of this study with reported studies on ion selective electrodes for Zn^{2+} ion is given in table 7. The repeatability and lifetime of the electrode was studied and it was successfully used in potentiometric titration as an indicator electrode for Zn^{2+} against EDTA.

ACKNOWLEDGEMENT
The authors are highly thankful to Dr. A. P. Majeed Khan, Chairman of Noorul Islam Centre for higher Education for providing with the facilities to undertake the work.

References

1. K. Kaur, R. Gupta, S. A. Saraf, and S. K. Saraf, *Compr. Rev. Food Sci. Food Saf.*, 13 (2014) 358.
2. T. M. Bray, and W. J. Bettger, *Free Radical Biol. Med.*, 8 (1990) 281.
3. A. S. Prasad, *J. Trace Elem. Med. Biol.*, 26 (2012) 66.

4. N. F. Shay, and H. F. Mangian, *J. Nutr.*, 130 (2000) 1493S.
5. A. S. Prasad, *Biochemistry of zinc*, Plenum Press, New York (1993).
6. S. Chandra, and D. R. Singh, *J. Saudi Chem. Soc.*, 14 (2010) 55.
7. S. R. Powell, *J. Nutr.*, 130 (2000) 1447S.
8. A. S. Prasad, B. Bao, F. W. J. Beck, O. Kucuk, and F. H. Sarkar, *Free Radical Biol. Med.*, 37 (2004) 1182.
9. M. P. Zago, and P. I. Oteiza, *Free Radical Biol. Med.*, 31 (2001) 266.
10. A. S. Prasad, *J. Trace Elem. Med. Biol.*, 28 (2014) 364.
11. A. Voegelin, S. Pfister, A. C. Scheinost, M. A. Marcus, and R. Kretzschmar, *Environ. Sci. Technol.*, 39 (2005) 6616.
12. J. Mertens, F. Degryse, D. Springael, and E. Smolders, *Environ. Sci. Technol.*, 41 (2007) 2992.
13. E. Callender, and K. C. Rice, *Environ. Sci. Technol.*, 34 (2000) 232.
14. C. R. T. Tarley, V. S. Santos, B. E. L. Baêta, A. C. Pereira, and L. T. Kubota, *J. Hazard. Mater.*, 169 (2009) 256.
15. M. Soylak, M. Tuzen, A. S. Souza, M. d. G. A. Korn, and S. L. C. Ferreira, *J. Hazard. Mater.*, 149 (2007) 264.
16. C. E. Säbel, J. M. Neureuther, and S. Siemann, *Anal. Biochem.*, 397 (2010) 218.
17. P. Jiang, and Z. Guo, *Coord. Chem. Rev.*, 248 (2004) 205.
18. L. Chew, D. Bradley, A. Y. Mohd, and M. M. Jamil, *Appl. Radiat. Isot.*, 53 (2000) 633.
19. M. A. Abbasi, Z. H. Ibupoto, M. Hussain, Y. Khan, A. Khan, O. Nur, and M. Willander, *Sensors*, 12 (2012) 15424.
20. U. Fiedler-Linnersund, and K. M. Bhatti, *Anal. Chim. Acta*, 111 (1979) 57.
21. M. Shamsipur, S. Rouhani, M. R. Ganjali, H. Sharghi, and H. Eshghi, *Sens. Actuators, B*, 59 (1999) 30.
22. M. Saleh, and A. Gaber, *Electroanalysis*, 13 (2001) 104.
23. V. Gupta, S. Agarwal, A. Jakob, and H. Lang, *Sens. Actuators, B*, 114 (2006) 812.
24. R. Kojima, and S. Kamata, *Anal. Sci.*, 10 (1994) 409.
25. I. M. Isa, S. M. Noor, Y. Juahir, N. Hashim, M. Ahmad, A. Kamari, A. Mohamed, S. Ab Ghani, and N. I. Wardani, *Int. J. Electrochem. Sci.*, 9 (2014) 4512.
26. M. Hosseini, S. D. Abkenar, M. Ganjali, and F. Faridbod, *Mater. Sci. Eng., C*, 31 (2011) 428.
27. Q. Fu, S. Qian, N. Li, Q. Xia, and Y. Ji, *Int. J. Electrochem. Sci.*, 7 (2012) 6799.
28. F. Mizani, and M. Ziaeiha, *Int. J. Electrochem. Sci.*, 7 (2012) 7770.
29. V. Gupta, D. Chauhan, V. Saini, S. Agarwal, M. Antonijevic, and H. Lang, *Sensors*, 3 (2003) 223.
30. H. Beitollahi, H. Karimi-Maleh, and H. Khabazzadeh, *Anal. Chem.*, 80 (2008) 9848.
31. H. Karimi-Maleh, P. Biparva, and M. Hatami, *Biosens. Bioelectron.*, 48 (2013) 270.
32. M. Elyasi, M. A. Khalilzadeh, and H. Karimi-Maleh, *Food Chem.*, 141 (2013) 4311.
33. I. Noviandri, and R. Rakhmana, *Int. J. Electrochem. Sci.*, 7 (2012)
34. P. M. Ajayan, *Chem. Rev.*, 99 (1999) 1787.
35. R. T. da Rocha, I. G. Gutz, and C. L. do Lago, *J. Chem. Educ.*, 72 (1995) 1135.
36. Y. Umezawa, K. Umezawa, and H. Sato, *Pure Appl. Chem.*, 67 (1995) 507.
37. M. Mourabet, A. El Rhilassi, H. El Boujaady, M. Bennani-Ziatni, and A. Taitai, *Arabian J. Chem.*, (2014) 10.1016/j.arabjc.2013.12.028.
38. M. Ghaedi, A. Asfaram, B. Mirtamizdoust, A. Bazrafshan, and S. Hajati, *RSC Adv.*, 5 (2015) 42376.
39. A. I. Khuri, and J. A. Cornell, *Response Surfaces : Designs and Analyses*, M. Dekker, New York (1996).
40. R. P. Buck, and E. Lindner, *Pure Appl. Chem.*, 66 (1994) 2527.
41. M. R. Ganjali, F. Faridbod, P. Norouzi, and M. Adib, *Sens. Actuators, B*, 120 (2006) 119.
42. M. R. Ganjali, P. Norouzi, A. Daftari, F. Faridbod, and M. Salavati-Niasari, *Sens. Actuators, B*, 120 (2007) 673.

43. V. Gupta, M. Al Khayat, A. Minocha, and P. Kumar, *Anal. Chim. Acta*, 532 (2005) 153.
44. V. K. Gupta, A. K. Jain, L. P. Singh, and U. Khurana, *Electrochim. Acta*, 43 (1998) 2047.
45. V. Gupta, R. Goyal, M. Al Khayat, P. Kumar, and N. Bachheti, *Talanta*, 69 (2006) 1149.
46. M. A. Akl, and M. H. A. El-Aziz, *Arabian J. Chem.*, (2011) 10.1016/j.arabjc.2011.09.009.
47. V. K. Gupta, *Sens. Actuators, B*, 55 (1999) 195.
48. P. Singh, A. K. Singh, and A. Jain, *Electrochim. Acta*, 56 (2011) 5386.
49. N. R. Gupta, S. Mittal, S. Kumar, and S. A. Kumar, *Mater. Sci. Eng., C*, 28 (2008) 1025.
50. V. Gupta, A. Kumar, and R. Mangla, *Sens. Actuators, B*, 76 (2001) 617.
51. A. Fakhari, M. Shamsipur, and K. Ghanbari, *Anal. Chim. Acta*, 460 (2002) 177.
52. S. K. Srivastava, V. K. Gupta, and S. Jain, *Anal. Chem.*, 68 (1996) 1272.
53. M. Gholivand, and Y. Mozaffari, *Talanta*, 59 (2003) 399.